Evaluation of the Mechanical Properties of the Samples Made by FDM 3D Printing

ALEXANDRU POPA*, NICOLAE FAUR*, MIHAI HLUSCU*, COSMIN BELIN*
Mechanics and Strength of Materials department, Politehnica University of Timisoara, 3 Victoriei Sq., 300006 Timisoara, Romania

Designing a sample to be made by FDM 3D printing is a fundamental problem in further studies related to such printed structures as material properties vary depending on filament orientation and G-code particularities. Samples designed to simulate wall structures inside 3D printed parts have been tested to allow separate evaluation of key components in such parts. Results show a very long plastic region in filaments without imperfections. As filament strands break steps of similar values appear in the reaction force measured by the machine.

Keywords: FDM 3d printing, filament, structure, strand

FDM 3D printing is the most accessible form of rapid prototyping. The evolution of this branch of rapid prototyping has been fast and inexpensive and it is still ongoing. The reason behind this phenomenon is the open-source nature of both the hardware and the software involved [1-3].

An interesting side effect of the accessibility to FDM 3D printing technology is the possibility of ad-hoc tinkering. There are numerous blogs and video channels dedicated to this topic and doing basic to complicated experiments [2-4].

In the academic world, papers on FDM 3D printing are mostly approaching the topic from the same point of view as they do any other form of rapid prototyping - a CNC machine that performs material addition [4-8]. This academic approach is also similar in machining (material removal). The reasoning behind this approach being that all of the above are CNC machines that either add or remove material. This reasoning is correct as any advance in CNC and related technologies will positively impact all the applications mentioned above.

In the case of FDM 3D printing, however, there are intricacies specific to this application that have not been studied in enough detail or isolated appropriately [2, 4, 6, 7]. Most of these intricacies stem from the fact that FDM 3D printed parts are rarely, in practice, solid objects [3, 9,10]. While we can produce parts and samples completely filled with material there is never a compelling reason to do so with this particular technology [11-13].

On the topic of appropriate isolation of intricacies is the lack of consistency on how the filament orientation should be in standard test specimens [9]. Filament orientations in FDM 3D printed parts are entirely decided by the G-Code optimization algorithm which means that a test specimen will not represent the real part [14]. Geometrical anisotropy is present in both real part and test sample, but it is different in one from the other [12, 13, 15]. The geometrical anisotropy resulting from filament orientation of an FDM 3D printed standard tensile test specimen is undefined in any standard [10, 15]. The tensile test specimen is not the only example here as any other test specimen will be undefined from this point of view when created by FDM 3D printing.

A better abstraction of FDM 3D printed parts is a shell of multiple filament thicknesses with an internal structure of 1 filament thickness as reinforcement to achieve the desired rigidity [9]. This paper describes and analyzes test specimens that can help quantify the properties of key structures found in an FDM 3D printed part.

Experiments parts

3D printing configuration and tools

For 3D printing the samples the FDM printer Leapfrog Bolt Pro [16] (Fig. 1) has been used. The material used was PLA Filament – RBX-PLA-BK092 'Black as Night' [17].

The printing parameters can be seen in Table 1. The choice is a balance between speed and accuracy [1].

Fig. 1. The FDM printer Leapfrog Bolt Pro

Test equipment

For testing and analyzing the 3D printed samples the following tools were used:

-Instron 5967 Dual Column Series mechanical testing machine [18] (Fig. 2)

-Leica DMS1000 digital microscope [19] (Fig. 2)

Samples

The first attempt at sample design was based on the ASTM D638 Specimen. It had been redesigned to be fit for 3D printing and to allow testing of two distinct morphological parts of FDM 3D printed components however the 3D printing process created stress concentrators in the parts due to the automatically generated G-Code

* email: alexandru.popa2@student.upt.ro; nicolae.faur@upt.ro; mihai.hluscu@upt.ro; cosmin.belin@student.upt.ro

Table 1
THE PRINTING PARAMETERS

Extruder	
Nozzle Diameter	0.35 mm
Extrusion Multiplier	0.95
Retraction Distance	2mm
Extra Restart Distance	0mm
Retraction Vertical Lift	0.4mm
Retraction Speed	3000 mm/min
Coasting Distance	0.29mm

Layer	
Primary Layer Height	0.24mm
Top Solid Layers	6
Bottom Solid Layers	5
Outline/Perimeter Shells	2
Outline Direction	Outside-in
First Layer Height	80%
First Layer Width	120%
First Layer Speed	50%

Infill	
Interior Fill Percentage	40%
Internal Fill Pattern	Rectilinear
External Fill Pattern	Rectilinear
Outline Overlap	40%
Infill Extrusion Width	150%
Minimum Infill Length	5mm
Combine Infill Every	1 layers
Internal Infill Angle Offsets	45°, -45°
External Infill Angle Offsets	45°, -45°

Speeds	
Default Printing Speed	3600 mm/min
Outline Underspeed	40%
Solid Infill Underspeed	80%
Support Structure Underspeed	80%
X/Y Axis Movement Speed	12000 mm/min
Z Axis Movement Speed	1002 mm/min
Adjust printing speed for layers below	15 sec
Allow speed reductions down to	20%

Temperature	
Right Extruder	210°C
Heated Bed	50°C

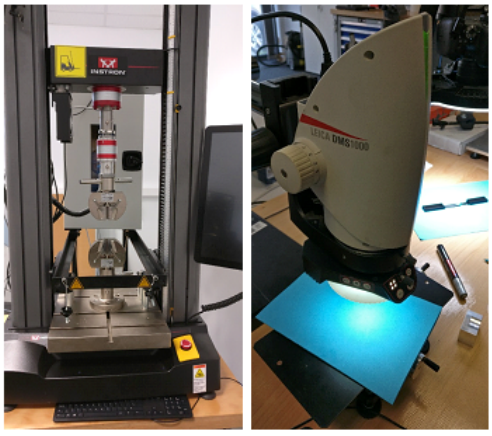

Fig. 2. Instron 5967 Dual Column Series testing machine and Leica DMS1000 Digital Microscope

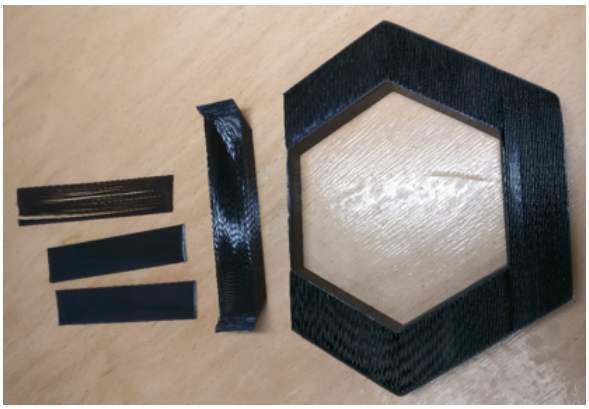

Fig. 3. Hexagonal 3D printed part with specimens cut out of it

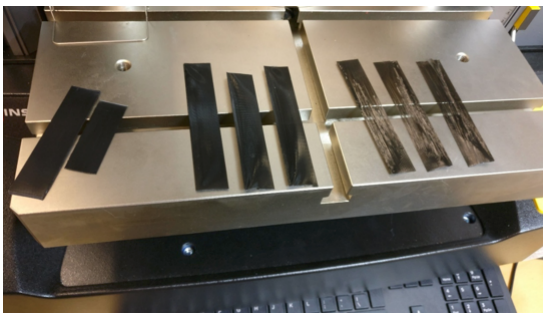

Fig. 4. Overview of cut out specimens

To overcome this issue a hexagon with dense structural walls was 3D printed and specimens were cut-out of the part (Fig. 3). The hexagon was designed to mimic a typical 3D printed part with structural walls as infill but with the particularity of parallelism between the walls to allow removal of individual pieces.

The cut-out specimens were 3 frayed structural walls (0.4mm, frayed due to printing defect), 3 structural walls (0.4mm, no defect), 1 external wall of 1 filament thickness (0.4mm) and 1 external wall of 2 filament thicknesses (0.8mm). These can be seen in figure 4.

Results and discussions

Table 2 contains the summary of the test results, including the relevant charts and reference data for all tested specimens.

The first observation, on the topic of 3D printed components, is the presence of weak points throughout the structure. Such weak points interfere with testing of the fused material and appear due to the printer nozzle changing directions [11-14]. An observable example of this phenomenon can be seen in figure 8. Due to the merging of 3 contours of filament the result in this particular case is the visible weak point between the thin wall and the tip of the solid part. This is the main reason behind the failure to test samples based on the ASTM D638 Specimen as strips of material cannot be attached properly to solid blocks of material. The drawback of testing strips of material is that shearing at the edge of the grippers has nullified half of the tests. To be noted that the strip seen below the weak point has been removed and tested separately with results equivalent to Sample 4.

The second observation is on the topic of frayed walls (Fig. 5). It can be seen in the successful tests that steps in force appear at the end of the test due to individual strands breaking. This phenomenon allows the measurement of the average tensile strength of a strand of fused filament without strengthening effects that can appear when the strands are also fused one to another. By analyzing the force steps starting from 57mm displacement until the end of the test (140mm) in figure 5, Sample 1 there can be measured 14 steps of approximately equal value. The average force drop between steps is 2.35N with the values being 2.1N; 2.4N; 2.2N; 2.1N; 3.3N; 2.5N; 2.1N; 2.1N; 2.3N; 2.5N; 2.2N; 2.7N; 2.3N; 2.1N. Considering that force variation is within +/- 0.1N on the same step we can assume that the average force drop represents the force at which a filament strand elongates in the plastic region of its strain-displacement curve. As they reach their maximum elongation in succession due to different lengths and gripping conditions strands snap creating the steps. The same measurement has been performed for figure 5, Sample 3 resulting in an average force of 2.16N from 9 steps with the values being 2.5N; 2.1N; 2.1N; 2.2N; 2.2N; 2.1N; 2.1N; 2.1N; 2.1N. The average of all values is 2.27N and this represents the average force at which a strand of filament extruded from a Ø0.4mm printer nozzle elongates in the plastic region of its strain-displacement curve.

The third observation, on the topic of normal walls, is the high elongation at constant force present in the successful tests done on one normal structural wall strip and one double filament thickness external wall. The behavior can be seen in figure 6, Sample 4 for the structural

Table 2
SUMMARY OF THE TEST RESULTS

Sample	Speed	Type	Chart	Notes during experiment
1	20mm/min	Frayed	Figure 5	Visible force steps as individual strands break
2	20mm/min	Frayed	Figure 5	Taped together for better machine gripping but slipped out of tape
3	20mm/min	Frayed	Figure 5	Visible force steps as individual strands break but many broken at initial pull
4	20mm/min	Normal	Figure 6	Specimen is elongating at constant force, ductile breaking
5	20mm/min	Normal	Figure 6	Shearing at machine gripping point, no conclusion
6	20mm/min	Normal	Figure 6	Shearing at machine gripping point, no conclusion
Strip	10mm/min	Normal	Figure 6	Strip preserved from failed attempt at the ASTM D638 Specimen. See Figures 8, 10. Elongated at constant force.
7	20mm/min	External 0.4mm	Figure 7	Shearing at machine gripping point, no conclusion
7	20mm/min	External 0.4mm	Figure 7	Repeat test on one remaining half. Shearing at machine gripping point, no conclusion
8	20mm/min	External 0.8mm	Figure 7	Shearing at machine gripping point, no conclusion
8	20mm/min	External 0.8mm	Figure 7	Repeat test on one remaining half. Specimen is elongating at constant force, ductile breaking.

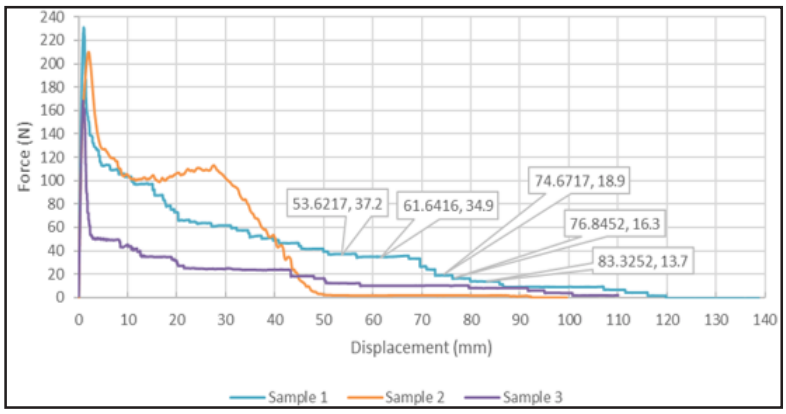

Fig.5. Frayed samples

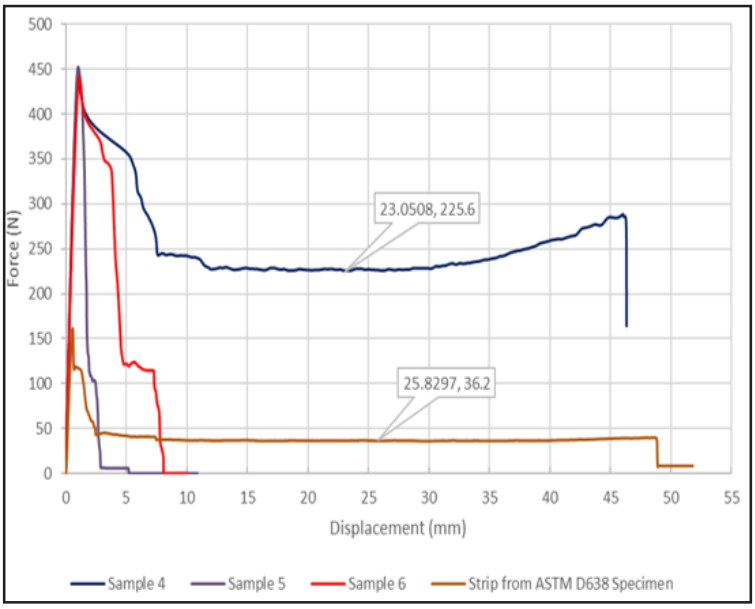

Fig.6 Normal samples

wall and figure 7, Sample 8_2 for the external wall. Figure 9 shows the visual aspect of the high elongation and allows the counting of filament strands fused in the strip.

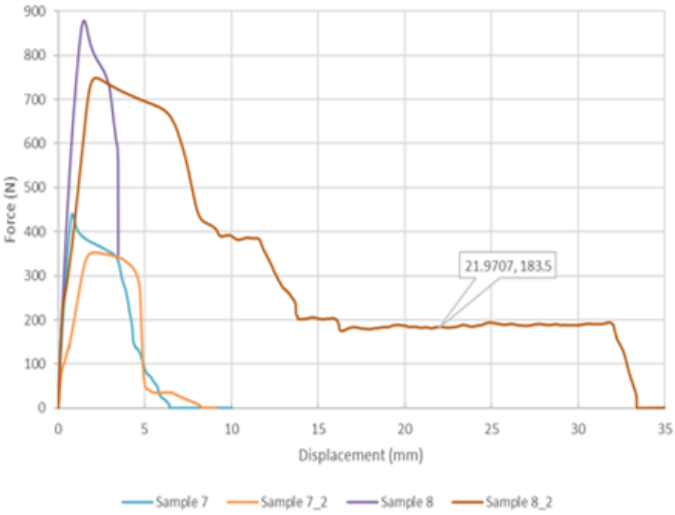

Fig.7 External walss

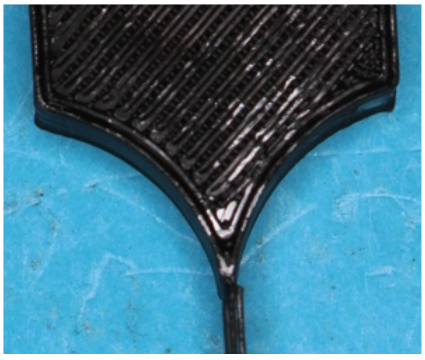

Fig. 8. Sample based on ASTM D638 with weak point

On visual inspection of Sample 4 after the test it can be observed that only the central region of the elongated strands was load bearing during the pass into the plastic region seen in figure 6. The two strands seen on the right side of the Sample 4 picture in figure 9 are not completely elongated and most likely represent the small dip in force observed at 12mm displacement. The average force recording between the displacement values of 15mm to 25mm is 226.9N. The load bearing region contains 81 strands, 79 of which are fused on two sides and 2 of which are fused only on one side. The cross-section of the strip is composed of 81 strands of filament and 80 fused connections between them. The average strand and corresponding fused connections elongate in the plastic region of their strain-displacement curve at 2.8N.

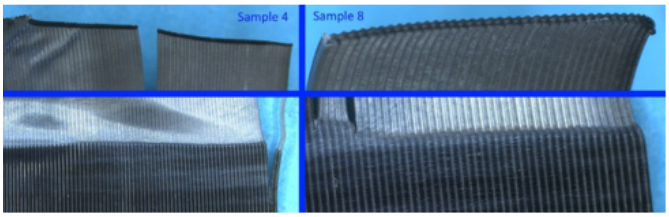

Fig. 9. Samples 4 (left) and 8 (right) after high plastic elongation

Similar results have been obtained from the strip removed from the ASTM D638 Specimen design attempt. The average force measured between 10mm to 30mm displacement on figure 6, ASTM D638 Specimen is 36.48N. The constant force measured between 49mm to 51mm displacement measured in the same graph is 8.3N and is given by a survivor strand which detached from the strip (fig. 10). The difference between these two averages is 28.18N which is the force at which the main part of the strip formed of 10 fused strands elongate in the plastic region of their strain-displacement curves. The average force per strand and corresponding fused connections is therefore 2.81N.

For Sample 8_2 the average of the registered constant force is 187.15N between 20mm and 30 mm displacement. The strand count on one side is 38 and therefore the total strand count in the elongated region is 76 fused filament strands. The average strand and corresponding fused connections elongate in the plastic region of their strain-displacement curve at 2.46N.

Conclusions

The strip samples are adequate for measuring filament strand properties due to successfully but inadequate for gripping in the testing machine. Using a higher number of samples can overcome this problem. Due to the presence of filament strands in all walls of an 3D FDM printed part it is possible to extract test samples and have comparable results from most such parts.

Strips and other structures composed of parallel filament strands act as multiple specimens being tested at the same time. This allows the reduction of sample sizes without skewing the results of statistical analyses. While advanced

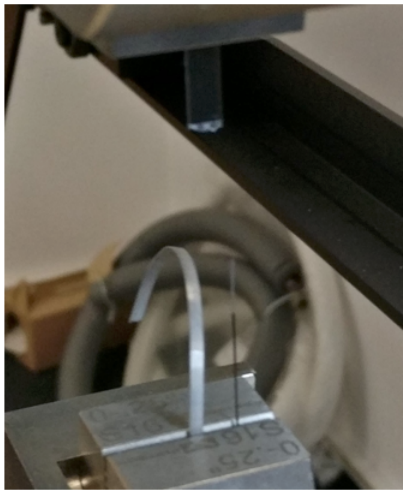

Fig. 10. Strip removed from ASTM D638 specimen (Fig. 8) after high plastic elongation

statistical analyses have not been performed in this paper there was enough raw data in the frayed sample tests to demonstrate the consistency of the breaking force of individual strands.

Filament strand properties were measured with the following results:

- elongation in the plastic region at constant force of 2.27N per standalone filament strand;
- elongation in the plastic region at constant force of 2.81N per fused strand in a wall of 1 filament strand thickness;
- elongation in the plastic region at constant force of 2.46N per fused strand in a wall of 2 filament strand thickness;
- while the average values given at point 2 are valid for the selected material and 3D printing parameters a more general conclusion is that a structural wall of fused filament strands can withstand a 23.8% higher load than its individual strands unfused.

A double wall of fused filament strands can withstand an 8.4% higher load than its individual strands unfused.

References

1.GALANTUCCI, L.M., BODI, I., KACANI, J., LAVECCHIA, F., Procedia Cirp, Vol. 28, 2014, p. 82

2.VASILESCU, M.D., FLESER, T., Influence of Technological Parametrson the Dimesion of Gear Parts Generated with PLA Matherial by FDM3D Printing, Mat Plast., **55** no. 2,, 2018, p. 247 -251

3.NEDELCU, D., COJOCARU, V., MICU, L.M., FLOREA, D., HLUSCU, M., Using of Polymers for Rapid Prototyping of an Axial Microturbine Runner and Wicked Gates, Mat. Plast. **56** , no.2, 2019, p.454-459

4.VASILESCU, M.D., Constructiv and Technological Consideration on the Generation of Gear Made by the DLP 3D-Printed Methode, Mat. Plast. **56**, no. 2, 2019, p.440-444

5.ANTON, L. E., BORDEASU, I., TABARA, I., Considerations regarding the use of EPO 99 B resin in manufacturing AXIAL hydraulic machinery runners, Mat. Plast. **45**, no. 2, 2008, p.190-192

6.POPESCU, A., ENCIU, G., DOBRESCU, T., PASCU, N. E., ExperimentalResearch Using the 3D Printing Technology with Plastic Materials for Prehension Systems Jaws, Mat Plast., **55**, no. 1, 2018, p.20-23

7.MITELEA, I., MICUL, L.M., BORDEASU, I., CRACIUNESCU, C.M., Journal of Materials Engineering and Performance, vol. 25, Issue 5, 2016, p.1939-1944

8.PRODAN, D., BUCURESTEANU, A., MOTOMANCEA, A., Constructionof Plastic Parts on CNC Engraving Machines and 3D Printers, Mat.Plast., **55,** no.1, 2018, p.75-78,

9.MOHAMED, O.A., MASOOD, S.H., BHOWMIK, J.L., Advances in Manufacturing, Vol. 3 Issue 1, 2015, p. 42

10.MASOOD, S.H., MAU, K., SONG, W.Q., Materials Science Forum, Vols. 654-656, 2010, p. 2556

11.ILIESCU, N., ATANASIU, C., HADAR, A., The simulation of the mechanical behaviour of engineering structures on models made of plastic materials with special properties, Mat. Plast. **42**, no. 1, 2005, p.72-76

12.TABACU, S., HADAR, A., MARINESCU, D., IVANESCU, M., BALASOIU, V., Numerical Procedures for the Improvement of the Structural Response of Thermoplastic Manufactured Parts,Mat. Plast. **46**, no. 2, 2010, p.192-197

13.MITELEA, I., BORDEASU, I., HADAR, A., Rev. Chim.(Bucharest), **56**, no. 11, 2005, p.1169-1174

14.BELLINI, A., GUCERI, S., Rapid Prototyping Journal, Vol. 9 Issue 4, 2003, p. 252

15.AHN, S.H., MONTERO, M., ODELL, D., ROUNDY, S., WRIGHT, P. K., Rapid Prototyping Journal, Vol. 8, Issue 4, 2002, p. 248

16.***https://www.lpfrg.com/products/leapfrog-bolt-pro/

17.***http://www.cel-robox.com/wp-content/uploads/MSDS/Robox%20SmartReel%20-%20PLA%20-%20All%20Colours%20-%20MSDS%20Ver1.4.pdf

18.***https://www.instron.com/-/media/literature-library/products/2013/02/5960-series-dual-column-tabletop-5kn-50kn.pdf?la=en

19.***https://downloads.leica-microsystems.com/Leica%20DMS1000/Brochures/Leica_ DMS1000%20Brochure_EN.pdf

Manuscript nreceived: 17.06.2019